applied sciences

MDPI

Article

The Potential of a Surface-Modified Titanium Implant with Tetrapeptide for Osseointegration Enhancement

Syamsiah Syam [1,2], Chia-Jen Wu [3,4,†], Wen-Chien Lan [5], Keng-Liang Ou [2,5,6,7,8], Bai-Hung Huang [2,9,10], Yu-Yeong Lin [11], Takashi Saito [7], Hsin-Yu Tsai [7], Yen-Chun Chuo [2,12], Ming-Liang Yen [13,*], Chung-Ming Liu [1,2,*] and Ping-Jen Hou [2,14]

1 Graduate Institute of Dental Science, College of Dentistry, China Medical University, Taichung 404, Taiwan; u108312101@cmu.edu.tw
2 Biomedical Technology R & D Center, China Medical University Hospital, Taichung 404, Taiwan; klou@tmu.edu.tw (K.-L.O.); T33782@mail.cmuh.org.tw (B.-H.H.); m249108001@tmu.edu.tw (Y.-C.C.); d825104002@tmu.edu.tw (P.-J.H.)
3 Department of Medical Imaging, Kaohsiung Medical University Hospital, Kaohsiung 807, Taiwan; 1020435@kmuh.org.tw
4 Department of Medical Imaging, Kaohsiung Municipal Ta-Tung Hospital, Kaohsiung Medical University, Kaohsiung 801, Taiwan
5 Department of Oral Hygiene Care, Ching Kuo Institute of Management and Health, Keelung 203, Taiwan; jameslan@ems.cku.edu.tw
6 Department of Dentistry, Taipei Medical University-Shuang Ho Hospital, New Taipei City 235, Taiwan
7 Division of Clinical Cariology and Endodontology, Department of Oral Rehabilitation, School of Dentistry, Health Sciences University of Hokkaido, Hokkaido 061-0293, Japan; t-saito@hoku-iryo-u.ac.jp (T.S.); m225098012@tmu.edu.tw (H.-Y.T.)
8 3D Global Biotech Inc. (Spin-Off Company from Taipei Medical University), New Taipei City 221, Taiwan
9 Asia Pacific Laser Institute, New Taipei City 220, Taiwan
10 Implant Academy of Minimally Invasive Dentistry, Taipei 106, Taiwan
11 J.U.S.T Dental Clinic, Taipei 114, Taiwan; just.dental@msa.hinet.net
12 School of Dental Technology, College of Oral Medicine, Taipei Medical University, Taipei 110, Taiwan
13 Division of Oral and Maxillofacial Surgery, Department of Dentistry, Taipei Medical University Hospital, Taipei 110, Taiwan
14 Graduate Institute of Biomedical Materials and Tissue Engineering, College of Biomedical Engineering, Taipei Medical University, Taipei 110, Taiwan
* Correspondence: 997184@h.tmu.edu.tw (M.-L.Y.); liuc@mail.cmu.edu.tw (C.-M.L.)
† Co-First author: Chia-Jen Wu.

check for updates

Citation: Syam, S.; Wu, C.-J.; Lan, W.-C.; Ou, K.-L.; Huang, B.-H.; Lin, Y.-Y.; Saito, T.; Tsai, H.-Y.; Chuo, Y.-C.; Yen, M.-L.; et al. The Potential of a Surface-Modified Titanium Implant with Tetrapeptide for Osseointegration Enhancement. *Appl. Sci.* **2021**, *11*, 2616. https://doi.org/10.3390/app11062616

Academic Editor: Gavriel Chaushu

Received: 2 February 2021
Accepted: 10 March 2021
Published: 15 March 2021

Abstract: In this study, the innovative dip-coating technique treated titanium (IDCT-Ti) implant with tetrapeptide Gly-Arg-Gly-Asp (GRGD) coating was investigated for its potential to enhance osseointegration. The L929 fibroblast cells were cultured in different concentrations of the GRGD (1%, 2%, and 5%). The cell viability was assessed through 3-[4,5-dimethylthiazol-2-yl]-2,5-diphenyltetrazolium bromide (MTT) assay and live/dead staining. The surface topography and nano-indentation were analyzed by atomic force microscopy. The hemocompatibility was evaluated via field-emission scanning electron microscopy, while contact angle analysis was detected by a goniometer. Radiograph evaluation was determined by panoramic imaging. It was found that the cell growth increased and had a survival rate of more than 70% in 1% GRGD. The mortality of L929 increased with the higher concentration of GRGD. The IDCT-Ti coated with 1% GRGD showed a nano-surface with a Young's modulus that was similar to human cortical bone, and it displayed greater red blood cell accumulations with abundant fibrin formation. As regards the wettability, the IDCT-Ti coated with 1% GRGD was lower than the SLA (sandblasted, large-grit, and acid-etched) treated implant. The X-ray image exhibited no bone loss around the implant at six months after placement. As a result, this study suggests that the IDCT-Ti implant, coated with 1% GRGD, has a tremendous likeliness to enhance osseointegration.

Keywords: tetrapeptide Gly-Arg-Gly-Asp; osseointegration; surface modification; dental implant

1. Introduction

The success rate of dental implants depends on osseointegration, which is initiated by cell adhesion when the implant surface meets the surrounding tissue [1–7]. Osseointegration failure is characterized by the instability or loosening of the implant, periimplantitis, and bone resorption [1,8–11]. Osseointegration is accomplished through two phases involving primary or mechanical stability, which is recognized after implant placement, and secondary or biological stability related to the healing process [12]. As such, it is crucial to perform various surface modifications to the implant where osseointegration occurs.

Dental implants generally use titanium (Ti) material, which has mechanical and biocompatible properties, yet these are insufficient to cause this material to be well-accepted and not considered as a foreign object, which leads to rejection by the body [9,10,13]. It is believed that the improvement of the mechanical, physical, and biological properties of the implant material, through surface modification, can overcome these obstacles to promote better bone contact to the implant surface, which in sequence can accelerate the osseointegration [14,15]. Of the various implant surface modifications, the sandblasted, large-grit, and acid-etched (SLA) surface treatment method is most often used to elevate the mechanical and physical properties of the implant, while biochemical methods can enhance the biological properties in the form of increased adhesion and cell migration by immobilization or delivery of various proteins, enzymes, or peptides on the implant surface [4,13,16,17].

The current study focuses on surface functionalization using peptides that allow the adhesion of cells to the implant surface, which has previously been treated by an innovative dip-coating technique (IDCT) [13]. In our previous study, surface modification with IDCT involved the application of polymer pluronic F127 (PF127), which acts as a scaffold with its amphiphilic properties and which not only improves wettability but also exhibits antibacterial action to induce the healing process [13,18]. However, the weak interaction with cells, and the lack of protein adsorption, were to be the shortcomings of the polymer that could have a negative impact on cell adhesion to the implant surface [16,19]. Several in vivo studies have displayed that type I collagen containing the amino acid sequence Arg-Gly-Asp (RGD) was useful to speed up fixation between the implant and the surrounding bone, and lead to the acceleration of osseointegration by enhancing cell adhesion, differentiation, and extracellular matrix (ECM) secretion [15,17]. Therefore, this study used Arg-Gly-Asp (RGD) peptide to mediate cell adhesion to the scaffold. The ability of RGD peptides to bind with integrin receptors leads to increased cell adhesion and its functions [6,20]. It was reported that the tetrapeptide Gly-Arg-Gly-Asp (GRGD) peptide sequence derived from fibronectins will bind to integrins and other ECM proteins [5]. Moreover, the GRGD peptide was also reported to be useful in modifying the Ti implant surface [21]. As mentioned above, the present study aimed to evaluate the IDCT-Ti implant coated with GRGD peptide in promoting osteoblast behavior to increase osseointegration.

2. Materials and Methods

2.1. Materials Preparation

The current study used a Ti dental implant that was surface-treated with IDCT as in our previously reported study [13]. Briefly, the IDCT process was performed by treating the Ti implant with SLA followed by coating the implant with PF127 [13]. The IDCT-Ti implant was then crosslinked with different concentrations of the GRGD peptide (1%, 2%, and 5%) through the dip-coating technique. This crosslinking process was carried out by soaking the IDCT-Ti implant for 15 min in the GRGD solution at 4 °C, and drying the samples in an oven with a maintained temperature of 30 °C for 5 h. For easy classification, the IDCT-Ti implants coated with 1%, 2%, and 5% GRGD are denoted as IDCT-Ti/GRGD-1, IDCT-Ti/GRGD-2, and IDCT-Ti/GRGD-5, respectively. The machined and SLA-treated Ti implant was adopted as a control for surface topography evaluation, the machined Ti implant for the hemocompatibility assay, and the SLA-treated implant for contact angle analysis.

2.2. Topography and Nano-Indentation Analysis

The Young's modulus on the surface of the tested implant was calculated by means of nano-indentation using a Berkovich diamond indenter tip (Asmec-UNAT-M, Dresden, Germany). The indentation experiments were operated under a 10 mN load of force for 5 s of hold time. An average of triplicates per sample was performed in the study. The high-resolution atomic force microscope (AFM; Nanoscope III D5000, Veeco Instruments Inc., Plainview, NY, USA) with a silicon probe working in tapping mode was applied to analyze the topography and post-nano-indentation features of the investigated samples. The investigated samples were captured with 512 pixel-resolution and the scan rate was 1 Hz.

2.3. Cell Culture and MTT Assay

The fibroblast cell line (L929, ATCC CCL-1, The Bioresource Collection and Research Center, Hsinchu, Taiwan) was used in this study. The L929 cells were plated in 3 sets of triplicates for each investigated sample, in a 24-well culture plate (1×10^4 cells per well density) with Dulbecco's modified Eagle minimum essential medium (DMEM, Gibco, Waltham, MA, USA), supplemented with 10% fetal bovine serum (FBS), 1% penicillin-streptomycin, and then incubated in a humidified 5% CO_2 incubator at 37 °C for 24 h. The tested GRGD peptides, over a range of concentrations (0% or control, 1%, 2%, and 5%), were added into the L929 cell culture wells and were incubated for an additional 24 h. After 24 h of incubation, 50 mL of 3-[4,5-dimethylthiazol-2-yl]-2,5-diphenyltetrazolium bromide (MTT, Sigma, Taipei, Taiwan) solution was added into each culture well and the culture plate was incubated for 4 h in a humidified atmosphere to form the formazan solvent precipitates. The precipitated formazan was solubilized in 150 mL of dimethyl sulfoxide (Sigma, Taipei, Taiwan), and absorbance was read at 595 nm using an Epoch microplate reader (BioTek Instruments Inc., Winooski, VT, USA). A short-term culturing experiment was used to investigate its acute cytotoxicity response according to ISO 10993-5 specification.

2.4. Cell Live/Dead Assay

The cell viability of L929 in different concentrations of GRGD peptide was evaluated via the live/dead kit after 24 h of incubation according to the manufacturer's instruction. Cells encapsulating the GRGD peptide were incubated at 25 °C for 30 min in a solution of 2.0 μM calcein acetoxymethyl ester (calcein-AM, Sigma, Taipei, Taiwan) to produce green fluorescence in live cells and 4.0 μM ethidium homodimer-1 (EthD-1; Sigma, Taipei, Taiwan) to produce red fluorescence in dead cells. Cell viability was subsequently observed through an FV1000/IX81 inverted fluorescence microscope (Olympus, Tokyo, Japan).

2.5. Contact Angle Analysis

The contact angle measurement of the investigated samples was analyzed using deionized water and blood by the sessile drop method and the immersion method, respectively. The sessile drop method was performed by dropping a 0.05 mL deionized water/blood droplet onto the investigated implant surface, maintaining a constant distance of 10 mm during the dropping process. Afterwards, the contact angle, meaning the angle that formed from the liquid droplets and the implant surface, was evaluated using a GBX digidrop goniometer (GBX Scientific LTD., Romans-sur-Isère, France). The immersion method was examined by bringing the apical part of the implant closer to the surface of the liquid (deionized water/blood) at a feed rate of 0.5 mm/s and it was immersed for 20 s. Finally, the immersion results were observed using a Phantom V310 digital high-speed camera (Vision Research Inc., Wayne, NJ, USA).

2.6. Hemocompatibility Assay

The hemocompatibility of the investigated sample was assessed using a 20 min red blood cells (RBC) morphology clotting time. Before being analyzed, the ethylene oxide was used to decontaminate the investigated samples within 24 h. After the sterilization process, the sample was put in a centrifuge tube with a capacity of 15 mL. Afterwards, the

investigated sample was dripped with 100 µL of blood, and allowed to coagulate at 37 °C for 20 min. The sample was then soaked in demineralized water at room temperature for 10 min to eliminate the uncoagulated blood that was found on the sample surface. Thereafter, the sample was fixed in 2% glutaraldehyde solution at 37 °C for 1h. The sample was then washed and rinsed with phosphate-buffer saline solution; air dried; and sputter coated with 25 nm of platinum films to enhance electrical conductivity. Subsequently, the investigated samples were analyzed using a JSM-6500 field-emission scanning electron microscope (FE-SEM; JEOL Ltd., Tokyo, Japan) operated at 25 kV.

2.7. Radiograph Evaluations In Vivo

The radiograph evaluation after implant placement was performed according to the clinical protocols that have been approved by the Taipei Medical University—Joint Institutional Review Board under the project identification code of TMU-JIRB 201301009, followed by ISO 1455 regulations. The dental implant (n = 15) was placed in 15 patients, following a one-stage surgery protocol. The surgical procedure was performed in standard aseptic surgical conditions. Local anesthesia was conducted on the site that was receiving the implant. Subsequently, a full-thickness crestal incision was made along the crest of the ridge, and elevated (Figure 1a). The implant was placed in the prepared osteotomy area and flap closure was performed by suturing around the implant without tension (Figure 1b). Finally, panoramic X-ray radiography was taken immediately and six months after placement.

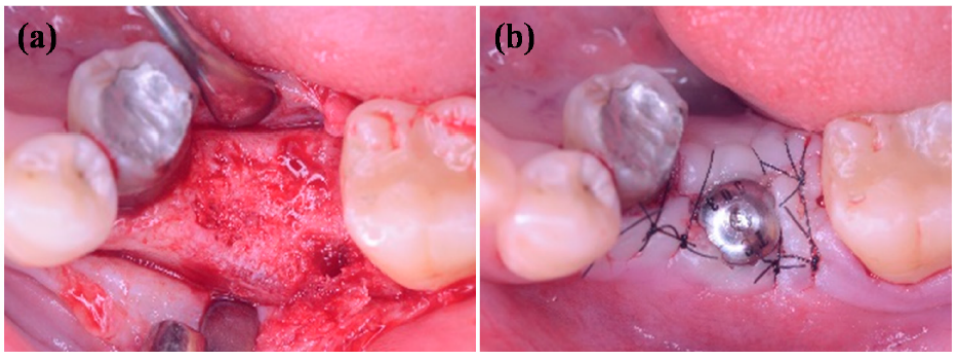

Figure 1. Surgical procedure of the investigated titanium (Ti) implant: (**a**) Full-thickness flap elevation and (**b**) dental implant placement.

2.8. Statistical Analysis

The statistical analysis with student's *t*-test function by SPSS software version 19.0 (SPSS Inc., Chicago, IL, USA) was applied in this study and determined as statistically significant at $p < 0.05$. All results were presented in means ± standard deviations.

3. Results

3.1. Comparisons of Surface Characteristic and Young's Modulus

The topography features of the machined, SLA-treated, and IDCT-Ti/GRGD-1 implants under AFM observation are displayed in Figure 2. Clearly, the machined surface implant exhibited a relatively smooth surface and some regions that were scratched as a consequence of the machining process (Figure 2a). The SLA-treated implant showed a rougher granular and irregular surface (Figure 2b), while the IDCT-Ti/GRGD-1 implant revealed a uniform nano-porous surface (as indicated by arrows, Figure 2c). Moreover, it was found that the Young's modulus of the machined, SLA-treated, and IDCT-Ti/GRGD-1 implants was 86.7 ± 3.1 GPa, 83.0 ± 1.4 GPa, and 28.7 ± 2.2 GPa, respectively. This result exhibited that the IDCT-Ti/GRGD-1 implant has a relatively low modulus of elasticity, which is closer to that of the host bone than other implants with various surface treatments. Similar results can also be found in the IDCT-Ti/GRGD-2 and IDCT-Ti/GRGD-3 implants.

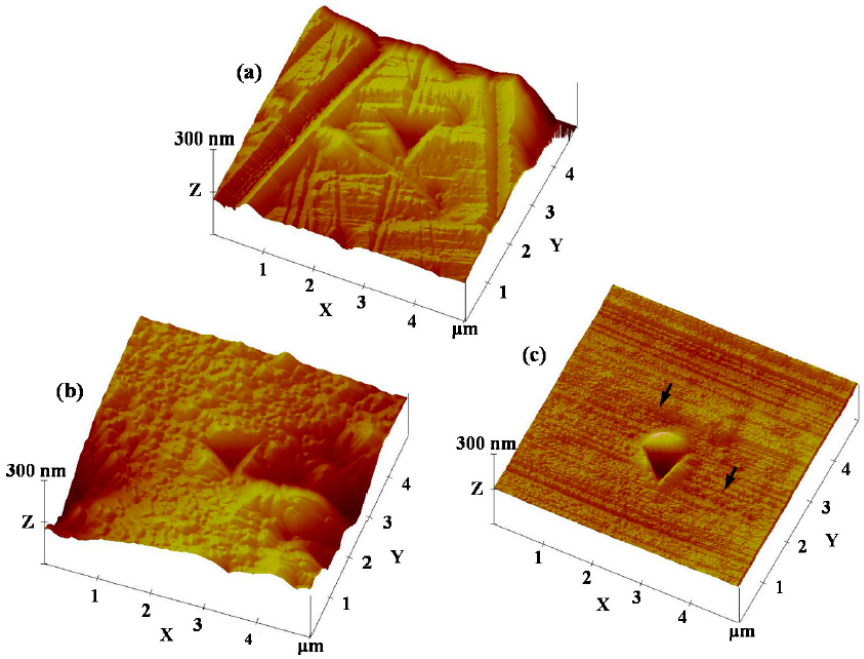

Figure 2. The topography features of the (**a**) machined, (**b**) sandblasted, large-grit, and acid-etched (SLA)-treated, and (**c**) IDCT-Ti implants coated with 1% Gly-Arg-Gly-Asp (IDCT-Ti/GRGD-1) implants under atomic force microscope (AFM) observation (5 μm × 5 μm).

3.2. Biocompatibility in Different Concentrations of the GRGD Peptide

Figure 3 illustrates the cell viability of L929 in different concentrations of the GRGD peptide for 24 h. It is obvious that the cell viability was increased by the 1% GRGD peptide and only the 1% GRGD peptide had a cell survival rate of more than 70%. Based on ISO 109993-5, it is considered an acute cytotoxic potential if the cell viability of the sample is reduced to <70% of the blank. Figure 4 shows that the lethality of L929 was raised with the increasing concentration of the GRGD peptide. After the L929 cells were exposed to higher concentrations of GRGD peptide for 24 h, it was revealed that the cells showed intolerance. This finding is in agreement with the results of the MTT assay.

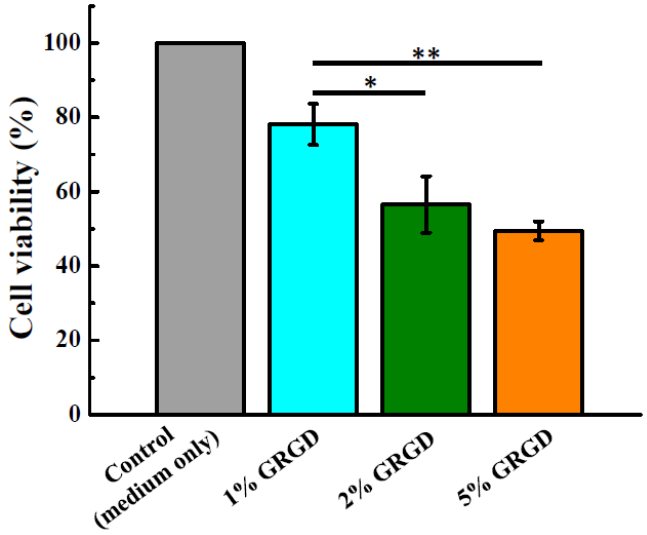

Figure 3. Effect of the GRGD peptide, with different concentrations, on the viability of L929 cell evaluated by 3-[4,5-dimethylthiazol-2-yl]-2,5-diphenyltetrazolium bromide (MTT) assay. (* $p < 0.05$ and ** $p < 0.01$).

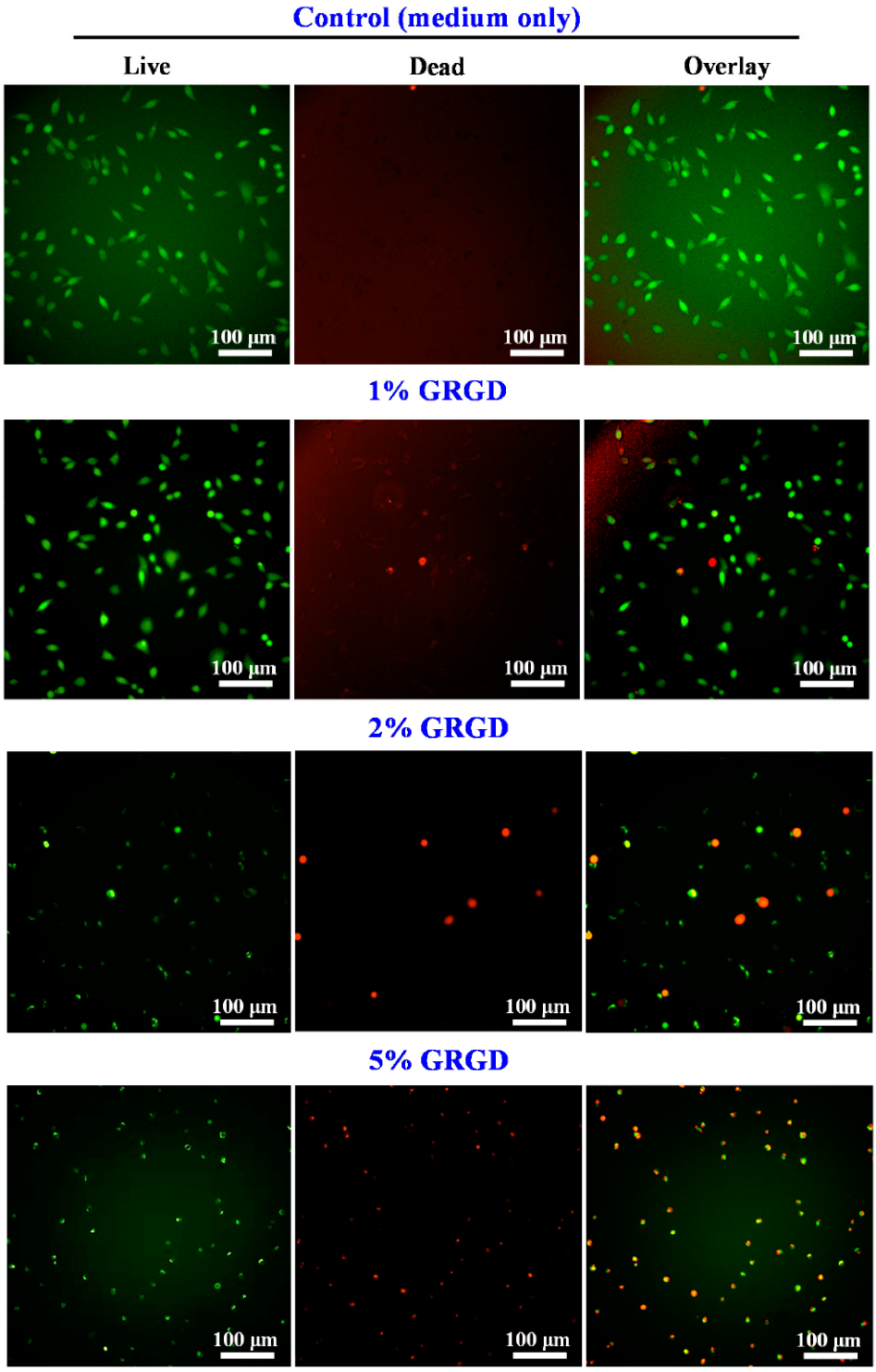

Figure 4. The result of the live/dead cell assay after the L929 cells were cultured in different concentrations of the GRGD peptide for 24 h. Magnification = 10×.

3.3. Wettability of the Investigated Implants

The wettability of the SLA-treated, and GRGD coated, IDCT-Ti implants was assessed by the dripping and immersion test as shown in Figure 5. The average contact angle in the dripping test for the SLA-treated implant was 75.5 ± 6.8° (deionized water, Figure 5a) and 135.1 ± 2.8° (blood, Figure 5b), while the IDCT-Ti/GRGD-1 implant in both deionized water and blood was nearly 0°. Furthermore, both deionized water and blood were raised along the thread of the IDCT-Ti/GRGD-1 implant to an average height of 2.5 ± 0.2 mm

and 3.0 ± 0.3 mm, after being immersed for 20 s, respectively. Obviously, both deionized water and blood appeared to be wetting and adhering to the IDCT-Ti/GRGD-1 implant as compared with the SLA-treated implant. A similar finding could also be observed when the Ti implant was subjected to a coat with a higher concentration of GRGD peptide (i.e., IDCT-Ti/GRGD-2 and IDCT-Ti/GRGD-3 implants).

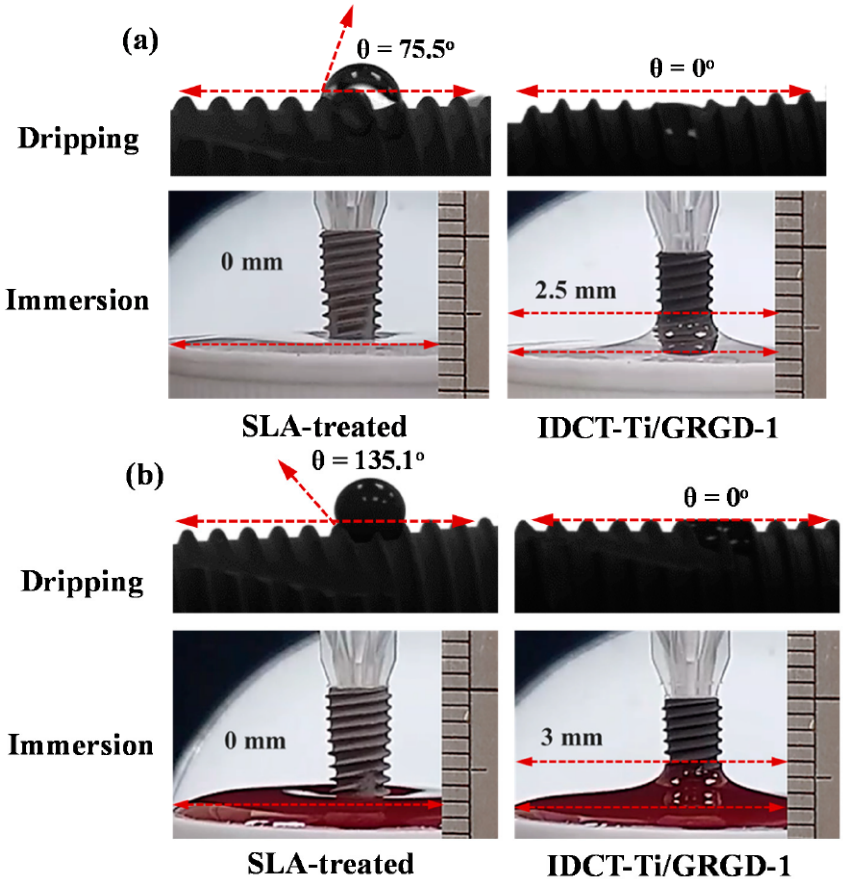

Figure 5. Wettability of the SLA-treated and IDCT-Ti/GRGD-1 implants under the dripping and immersion test: (**a**) deionized water test and (**b**) blood test.

3.4. Hemocompatibility of the Investigated Implants

Figure 6 shows the FE-SEM of RBC morphology for the untreated Ti implant and IDCT-Ti/GRGD-1 implant. Apparently, the untreated Ti implant exhibited less RBC accumulation (Figure 6a) than the IDCT-Ti/GRGD-1 implant surface. Figure 6b depicts an RBC trapped in abundant fibrin (as indicated by arrows) which is crucial in the wound-healing process.

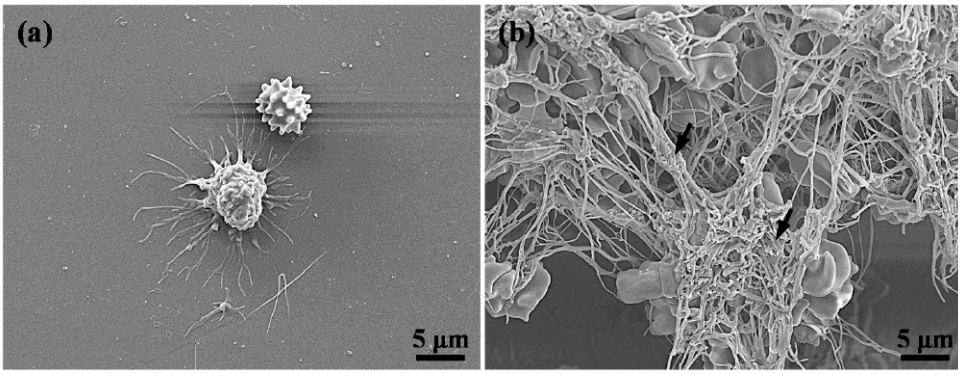

Figure 6. The FE-SEM images of RBC morphology on the (**a**) untreated Ti implant and (**b**) IDCT-Ti/GRGD-1 implant.

3.5. Radiograph Evaluations of the IDCT-Ti/GRGD-1 Implant

The panoramic view obtained from the IDCT-Ti/GRGD-1 implant, immediately and six months after placement, as shown in Figure 7. This figure represents the placement of the IDCT-Ti/GRGD-1 implant in the following different sites in the jawbone: Figure 7a as representative of implant placement in the mandibular region; Figure 7b for the maxillary region; and Figure 7c for the maxillary and mandibular region. Based on the results of the panoramic image, no bone loss was found after 6 months of implant placement, which indicates a supportive osseointegration around the implant.

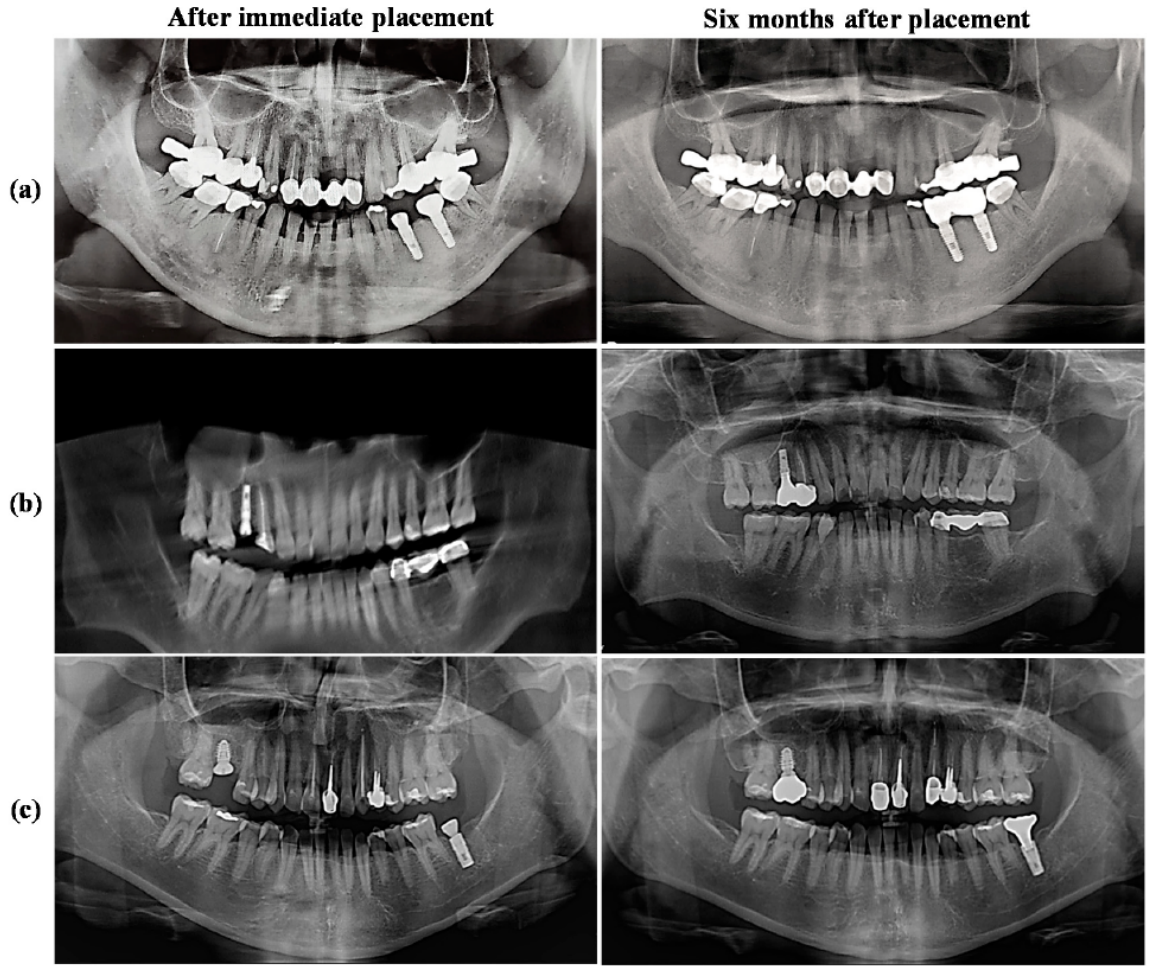

Figure 7. The panoramic of IDCT-Ti/GRGD-1 implant in (**a**) mandibular, (**b**) maxillary, and (**c**) maxillary and mandibular region, immediately and six months after placement. Note: figure (**b**) after immediate implant placement is the picture that was reconstructed from the cone-beam computed tomography.

4. Discussion

Surface modification of dental implants is essential in increasing the interaction between the implant and the surrounding bone, which will affect the osseointegration through the increasing number of cells adhering to the surface of the implant. The IDCT-Ti implants, coated with GRGD peptide, allow the increase in osteoblast adhesion and proliferation. The formation of bone around a foreign object such as an implant is a very complicated process. Both implants and substances that induce bone formation must function to support one another. Dental implants based on titanium are carriers of substances that can increase bone formation, and have characteristics that include high biocompatibility, good mechanical properties, can be combined with various inducing factors for bone formation, and do not inhibit bone formation induced by inducing factors [22]. The IDCT-Ti itself has facilitated the implant surface to simulate the ECM, which is crucial for cell attachment [13]. The

peptide represents a small part of the protein that is responsible for intercellular and ECM adhesion, while RGD is a peptide motif found in ECM proteins whose adhesion is integrin-mediated [11,23]. The ECM consists of various cell identification motifs such as fibronectin, vitronectin, laminin, collagen I, and bone sialoprotein, whereas the small peptide only provides a single motif [16,24–26]. Hence, the RGD peptide motif can selectively determine the type of cell adhesion receptor [16]. As a sequence of RGD, the GRGD peptide was reported to bind mostly to osteoblast cell activity [21].

The increase in GRGD peptide concentration appears to be directly proportional to cell death. Accordingly, GRGD in low concentrations emerges to be the best option for modifying the implant surface. This finding matches with our earlier study that also used low concentrations of GRGD to increase the adherence of fibroblast cells, and human hair follicle-derived mesenchymal stem cells [19]. Interestingly, not all RGD sequences show this phenomenon. Possible reasons for cell death include: (1) Cells have several integrin binding-receptors to RGD. If the binding receptors are related to the activation of the apoptotic response, there will be differences in cell sensitivity to RGD and its sequence. Conversely, if the binding is unrequired, the integrin receptor can still bind to peptides. (2) Osteoblast cells are sensitive to GRGD sequences, and in high concentrations they can cause loss of cell viability. (3) Peptide concentrations are associated with the formation of a peptide solution. The increase in peptide solution causes elevation in the detachment rate of focal adhesions at the back of the cell, which will increase cell migration and prevent cell reconvene [27,28].

The surface topography of the implant also affects cell characteristics. The nano-surface will alter the adhesion, motility, spread, proliferation, and differentiation of cells [1,10,29,30]. The nano-surface can also influence cell adhesion selectively, which is why osteoblast adhesion was more than fibroblast [30]. The topography of the implant also affects its success, not only in terms of cell adhesion but more towards the stability of the implant itself. Bone loss is one of the signs of implant failure, the major cause of which is excessive stress, while after insertion and when the implant is starting its functioning, it will be subject to various pressures [31–33]. Therefore, the implant should transfer the stress to the surrounding bone fairly. A study shows that threaded dental implants produce twice the stress of implants with a porous surface [34]. In the present study, the IDCT-Ti/GRGD-1 implant exhibited a uniform nano-porous surface. This condition is formed from surface modification with a polymer [35–38]. Furthermore, the nano-surface is known to transfer stress uniformly [34]. The main problem when implants replace missing teeth is that their mechanical properties are not identical with the bone and the teeth being replaced. Implants with higher elastic modulus will adsorb all the load, which creates a stress shielding effect and leads to bone loss [33]. According to the nano-indentation analysis, the Young's modulus of the IDCT-Ti/GRGD-1 surface was equivalent to cortical bone (~20 GPa), which would reduce the stiffness of the implant and prevent bone resorption around the implant [13,33,39].

The hemocompatibility assay of the IDCT-Ti/GRGD-1 implant revealed that the amount of RBC aggregation accompanied the presence of copious fibrin. This result is markedly different from our previous study using IDCT surface-modified implants without peptide involvement. The IDCT-Ti implant had less fibrin than the IDCT-Ti/GRGD-1 implant [13]. Fibronectin is required by fibrinogen to assemble in the ECM [40]. The presence of fibrinogen will cause the ECM to mediate cell migration and restore the matrix during tissue repair [21]. Fibrin will support the wound healing process, both soft and hard tissues, which will consequentially affect the osseointegration [7,41]. The soft tissue healing will create a physical seal on the bone around the implant, protecting from oral environment contamination such as bacteria [41]. Since implant placement causes injury in the jawbone, it will induce wound healing as hemostasis and coagulation, granulation of tissue formation, bone formation, and remodeling [42].

The good hemocompatibility is related to the wettability, which allows the absorption of various biological fluids, proteins, and cells [13,29]. The wettability of the IDCT-Ti/GRGD-1 implant using a water test is in line with our previous study, which was

obtained from the involvement of super hydrophilic PF127 on the surface-modified implant with IDCT [13]. In the current study, the wettability measurement was not only performed using deionized water, but also using blood. Both fluids have a different viscosity, with a blood viscosity (3.49 cPo) higher than water (1 cPo) [43]. Indeed, lower viscosities are more absorbable compared to higher viscosities. Moreover, blood is the fluid that first makes contact with the implant, and the osseointegration begins [43–45]. A surface is hydrophilic if it has a contact angle of less than 90°, super hydrophilic if it approaches 0°, while a surface is hydrophobic if the contact angle exceeds 90°, and superhydrophobic if it is higher than 150° [46,47]. The present study has found that the contact angle pattern of blood is similar to water, which is close to 0°. The SLA implant reveals hydrophilic surface properties when subjected to a water test, whereas when using blood, the SLA implant is almost superhydrophobic. Contrarily, another study also used blood to assess the wettability, and it was found that the contact angle at the SLA-treated implant was about 27° [44]. The difference in results may be due to the measurement of the contact angle performed on flat discs, which cannot represent the actual implant surface [46,47]. Furthermore, wettability is closely related to surface energy; a lower contact angle indicates high surface energy, which means it can allow the liquid to spread and adhere more widely to the implant surface [47,48].

Osseointegration can be assessed through intraosseous implant stability using X-ray [14,49]. In this study, the absence of radiolucency as a sign of bone resorption surrounding the implant demonstrates the stability of the intraosseous implant that was observed 6 months after placement. The quality and quantity of bone, and the location of implant placement in the jaw, also determines the success of the dental implant [50]. The bone quality in the posterior maxilla is lower than in the mandibular [51]. Hence, the survival rate for the implant that was placed in the maxilla is lower than that in the mandibular [7,52]. In our study, the implant placement in both maxilla and mandibular showed good stability, indicating satisfactory osseointegration. Accordingly, the GRGD-coated IDCT-Ti dental implants could be favorable for bone tissue regeneration, which promotes prosperous dental implants. Finally, additional research needs to be carried out to corroborate the bone healing and osseointegration potential of the GRGD-coated IDCT-Ti dental implant in terms of clinical application with a greater sample size, as well as various and longer follow-up periods.

5. Conclusions

The surface modification with GRGD peptide was performed on the IDCT-Ti implant. It was found that there was a positive impact on the implant surface characteristics, comprising topography, hemocompatibility, and wettability, which are related to increased adhesion of osteoblast cells on the IDCT-Ti/GRGD-1 implant surface, and leads to osseointegration. These results have been supported by the absence of radiolucency, indicating non-appearance of bone loss around the implant on the radiographic examination six months after implant placement.

Author Contributions: Writing—original draft, S.S.; investigation, S.S. and C.-J.W.; data curation, Y.-C.C. and H.-Y.T.; methodology, B.-H.H. and W.-C.L.; supervision, K.-L.O. and T.S.; resources, Y.-Y.L.; validation, P.-J.H.; writing—review and editing, M.-L.Y. and C.-M.L. All authors have read and agreed to the published version of the manuscript.

Funding: This research received no external funding.

Institutional Review Board Statement: The study was conducted according to the guidelines of the Declaration of Helsinki, and approved by the Taipei Medical University—Joint Institutional Review Board (TMU-JIRB 201301009).

Informed Consent Statement: Informed consent was obtained from all subjects involved in the study. Written informed consent has been obtained from the patients to publish this paper.

Data Availability Statement: Data is contained within the article.

Acknowledgments: The authors would like to thank the T-Plus Implant Tech. Co., Ltd. for technical support.

Conflicts of Interest: The authors declare no conflict of interest in this work.

References

1. Li, Y.; You, Y.; Li, B.; Song, Y.; Ma, A.; Chen, B.; Han, W.; Li, C. Improved cell adhesion and osseointegration on anodic oxidation modified titanium implant surface. *J. Hard Tissue Biol.* **2019**, *28*, 8. [CrossRef]
2. Albertini, M.; Fernandez-Yague, M.; Lazaro, P.; Herrero-Climent, M.; Rios-Santos, J.V.; Bullon, P.; Gil, F.J. Advances in surfaces and osseointegration in implantology. Biomimetic surfaces. *Med. Oral Patol. Oral Cir. Bucal* **2015**, *20*, e316–e325. [CrossRef] [PubMed]
3. Alves, S.F.; Wassall, T. In vitro evaluation of osteoblastic cell adhesion on machined osseointegrated implants. *Braz. Oral Res.* **2009**, *23*, 6. [CrossRef] [PubMed]
4. Kim, M.H.; Park, K.; Choi, K.H.; Kim, S.H.; Kim, S.E.; Jeong, C.M.; Huh, J.B. Cell adhesion and in vivo osseointegration of sandblasted/acid etched/anodized dental implants. *Int. J. Mol. Sci.* **2015**, *16*, 10324–10336. [CrossRef] [PubMed]
5. Molina, N.; Gonzalez, A.; Monopoli, D.; Mentado, B.; Becerra, J.; Santos-Ruiz, L.; Vida, Y.; Perez-Inestrosa, E. Dendritic scaffold onto titanium implants. A versatile strategy increasing biocompatibility. *Polymers* **2020**, *12*, 770. [CrossRef]
6. Park, S.-Y.; Kim, H.-S.; Kim, J.-H.; Shim, J.-H.; Yun, M.-J.; Jeon, Y.-C.; Huh, J.-B.; Jeong, C.-M. Effects of anodized titanium implant coated with RGD peptides via chemical fixation on osseointegration and bone regeneration. *Tissue Eng. Regen. Med.* **2012**, *9*, 194–202. [CrossRef]
7. Feller, L.; Chandran, R.; Khammissa, R.A.; Meyerov, R.; Jadwat, Y.; Bouckaert, M.; Schechter, I.; Lemmer, J. Osseointegration: Biological events in relation to characteristics of the implant surface. *SADJ* **2014**, *69*, 6.
8. Likibi, F.; Jiang, B.; Li, B. Biomimetic nanocoating promotes osteoblast cell adhesion on biomedical implants. *J. Mater. Res.* **2011**, *23*, 3222–3228. [CrossRef]
9. Chen, X.; Zhou, X.C.; Liu, S.; Wu, R.F.; Aparicio, C.; Wu, J.Y. In vivo osseointegration of dental implants with an antimicrobial peptide coating. *J. Mater. Sci. Mater. Med.* **2017**, *28*, 76. [CrossRef]
10. Damiati, L.; Eales, M.G.; Nobbs, A.H.; Su, B.; Tsimbouri, P.M.; Sameron-Sanchez, M.; Dalby, M.J. Impact of surface topography and coating on osteogenesis and bacterial attachment on titanium implants. *J. Tissue Eng.* **2018**, *9*, 16. [CrossRef]
11. Agarwal, R.; Garcia, A.J. Biomaterial strategies for engineering implants for enhanced osseointegration and bone repair. *Adv. Drug Deliv. Rev.* **2015**, *94*, 53–62. [CrossRef] [PubMed]
12. Chiang, H.J.; Hsu, H.J.; Peng, P.W.; Wu, C.Z.; Ou, K.L.; Cheng, H.Y.; Walinski, C.J.; Sugiatno, E. Early bone response to machined, sandblasting acid etching (SLA) and novel surface-functionalization (SLAffinity) titanium implants: Characterization, biomechanical analysis and histological evaluation in pigs. *J. Biomed. Mater. Res. A* **2016**, *104*, 397–405. [CrossRef] [PubMed]
13. Hou, P.-J.; Syam, S.; Lan, W.-C.; Ou, K.-L.; Huang, B.-H.; Chan, K.-C.; Tsai, C.-H.; Saito, T.; Liu, C.-M.; Chou, H.-H.; et al. Development of a surface-functionalized titanium implant for promoting osseointegration: Surface characteristics, hemocompatibility, and in vivo evaluation. *Appl. Sci.* **2020**, *10*, 8582. [CrossRef]
14. Zanetti, E.M.; Pascoletti, G.; Cali, M.; Bignardi, C.; Franceschini, G. Clinical assessment of dental implant stability during follow-up: What is actually measured, and perspectives. *Biosensors* **2018**, *8*, 68. [CrossRef]
15. Scarano, A.; Lorusso, F.; Orsini, T.; Morra, M.; Iviglia, G.; Valbonetti, L. Biomimetic surfaces coated with covalently immobilized collagen type I: An X-ray photoelectron spectroscopy, atomic force microscopy, micro-CT and histomorphometrical study in rabbits. *Int. J. Mol. Sci.* **2019**, *20*, 724. [CrossRef]
16. Hersel, U.; Dahmen, C.; Kessler, H. RGD modified polymers: Biomaterials for stimulated cell adhesion and beyond. *Biomaterials* **2003**, *24*, 4385–4415. [CrossRef]
17. Morra, M.; Cassinelli, C.; Meda, L.; Fini, M.; Giavaresi, G.; Giardino, R. Surface analysis and effects on interfacial bone microhardness of collagen-coated titanium implants: A rabbit model. *Int. J. Oral Maxillofac. Implant.* **2005**, *20*, 8.
18. Dogan, A.; Yalvac, M.E.; Sahin, F.; Kabanov, A.V.; Palotas, A.; Rizvanov, A.A. Differentiation of human stem cells is promoted by amphiphilic pluronic block copolymers. *Int. J. Nanomed.* **2012**, *7*, 4849–4860. [CrossRef]
19. Cho, Y.-C.; Huang, H.-T.; Lan, W.-C.; Huang, M.-S.; Saito, T.; Huang, B.-H.; Tsai, C.-H.; Fan, F.-Y.; Ou, K.-L. The potential of a tailored biomimetic hydrogel for in vitro cell culture applications: Characterization and biocompatibility. *Appl. Sci.* **2020**, *10*, 9035. [CrossRef]
20. Zheng, Y.; Xiong, C.; Li, X.; Zhang, L. Covalent attachment of cell-adhesive peptide Gly-Arg-Gly-Asp (GRGD) to poly(etheretherketone) surface by tailored silanization layers technique. *Appl. Surf. Sci.* **2014**, *320*, 93–101. [CrossRef]
21. Abiko, Y.; Pugdee, K.; Hirai, T.; Chu, C.-H.; Ando, T.; Shibata, Y. Attachment activity of RGD-motif peptides to osteoblast-like cell line MC3T3-E1. *Int. J. Oral Med. Sci.* **2007**, *6*, 3. [CrossRef]
22. Piattelli, A.; Scarano, A.; Corigliano, M.; Piattelli, M. Effects of alkaline phosphatase on bone healing around plasma-sprayed titanium implants: A pilot study in rabbits. *Biomaterials* **1996**, *17*, 7. [CrossRef]
23. Feller, L.; Jadwat, Y.; Khammissa, R.A.; Meyerov, R.; Schechter, I.; Lemmer, J. Cellular responses evoked by different surface characteristics of intraosseous titanium implants. *Biomed. Res. Int.* **2015**, *2015*, 171945. [CrossRef]
24. Lebaron, R.G.; Athanasiou, K.A. Extracellular matrix cell adhesion peptides: Functional applications in orthopedic materials. *Tissue Eng.* **2000**, *6*, 19. [CrossRef] [PubMed]

25. Hennessy, K.M.; Clem, W.C.; Phipps, M.C.; Sawyer, A.A.; Shaikh, F.M.; Bellis, S.L. The effect of RGD peptides on osseointegration of hydroxyapatite biomaterials. *Biomaterials* **2008**, *29*, 19. [CrossRef] [PubMed]
26. Bellis, S.L. Advantages of RGD peptides for directing cell association with biomaterials. *Biomaterials* **2011**, *32*, 4205–4210. [CrossRef] [PubMed]
27. Shabbir, S.H.; Eisenberg, J.L.; Mrksich, M. An inhibitor of a cell adhesion receptor stimulates cell migration. *Angew. Chem. Int. Ed. Engl.* **2010**, *49*, 7706–7709. [CrossRef] [PubMed]
28. Perlot, R.L., Jr.; Shapiro, I.M.; Mansfield, K.; Adams, C.S. Matrix regulation of skeletal cell apoptosis II: Role of Arg-Gly-Asp-containing peptides. *J. Bone Miner. Res.* **2002**, *17*, 11. [CrossRef] [PubMed]
29. Pachauri, P.; Bathala, L.R.; Sangur, R. Techniques for dental implant nanosurface modifications. *J. Adv. Prosthodont.* **2014**, *6*, 498–504. [CrossRef] [PubMed]
30. Thakral, G.; Thakral, R.; Sharma, N.; Seth, J.; Vashisht, P. Nanosurface—The future of implants. *J. Clin. Diagn. Res.* **2014**, *8*, ZE07–ZE10. [CrossRef] [PubMed]
31. Ogle, O.E. Implant surface material, design, and osseointegration. *Dent. Clin. N. Am.* **2015**, *59*, 505–520. [CrossRef]
32. Cheng, H.Y.; Chu, K.T.; Shen, F.C.; Pan, Y.N.; Chou, H.H.; Ou, K.L. Stress effect on bone remodeling and osseointegration on dental implant with novel nano/microporous surface functionalization. *J. Biomed. Mater. Res. A* **2013**, *101*, 1158–1164. [CrossRef]
33. Brizuela, A.; Herrero-Climent, M.; Rios-Carrasco, E.; Rios-Santos, J.V.; Perez, R.A.; Manero, J.M.; Gil Mur, J. Influence of the elastic modulus on the osseointegration of dental implants. *Materials* **2019**, *12*, 980. [CrossRef] [PubMed]
34. Hou, P.J.; Ou, K.L.; Wang, C.C.; Huang, C.F.; Ruslin, M.; Sugiatno, E.; Yang, T.S.; Chou, H.H. Hybrid micro/nanostructural surface offering improved stress distribution and enhanced osseointegration properties of the biomedical titanium implant. *J. Mech. Behav. Biomed. Mater.* **2018**, *79*, 173–180. [CrossRef]
35. Wennerberg, A.; Jimbo, R.; Stubinger, S.; Obrecht, M.; Dard, M.; Berner, S. Nanostructures and hydrophilicity influence osseointegration: A biomechanical study in the rabbit tibia. *Clin. Oral Implant. Res.* **2014**, *25*, 1041–1050. [CrossRef] [PubMed]
36. Wennerberg, A.; Galli, S.; Albrektsson, T. Current knowledge about the hydrophilic and nanostructured SLActive surface. *Clin. Cosmet. Investig. Dent.* **2011**, *3*, 59–67. [CrossRef] [PubMed]
37. Yeo, I.L. Modifications of dental implant surfaces at the micro- and nano-level for enhanced osseointegration. *Materials* **2019**, *13*, 89. [CrossRef]
38. Shibli, J.A.; Ehrenfest, D.D. In dental implant surface, NanoWar has begun, but NanoQuest is still at stake. *POSEIDO J.* **2013**, *1*, 10.
39. Sargeant, T.D.; Guler, M.O.; Oppenheimer, S.M.; Mata, A.; Satcher, R.L.; Dunand, D.C.; Stupp, S.I. Hybrid bone implants: Self-assembly of peptide amphiphile nanofibers within porous titanium. *Biomaterials* **2008**, *29*, 161–171. [CrossRef]
40. Pereira, M.; Rybarczyk, B.J.; Odrljin, T.M.; Hocking, D.C.; Sottile, J.; Simpson-Haidaris, P.J. The incorporation of fibrinogen into extracellular matrix is dependent on active assembly of a fibronectin matrix. *J. Cell Sci.* **2002**, *115*, 9.
41. Villar, C.C.; Huynh-Ba, G.; Millis, M.P.; Cochran, D.L. Wound healing around dental implants. *Endod. Top.* **2012**, *25*, 19.
42. Bosshardt, D.D.; Chappuis, V.; Buser, D. Osseointegration of titanium, titanium alloy and zirconia dental implants: Current knowledge and open questions. *Periodontol. 2000* **2017**, *73*, 19. [CrossRef] [PubMed]
43. Torrisi, L.; Scolaro, C. Blood wettability of haemocompatible carbon-based materials. *J. Adv. Chem. Eng.* **2017**, *7*, 1000179. [CrossRef]
44. Koca, R.B.; Guven, O.; Celik, M.S.; Firatli, E. Wetting properties of blood lipid fractions on different titanium surfaces. *Int. J. Implant Dent.* **2020**, *6*, 16. [CrossRef] [PubMed]
45. Traini, T.; Murmura, G.; Sinjari, B.; Perfetti, G.; Scarano, A.; D'Arcangelo, C.; Caputi, S. The surface anodization of titanium dental implants improves blood clot formation followed by osseointegration. *Coatings* **2018**, *8*, 252. [CrossRef]
46. Gittens, R.A.; Scheideler, L.; Rupp, F.; Hyzy, S.L.; Geis-Gerstorfer, J.; Schwartz, Z.; Boyan, B.D. A review on the wettability of dental implant surfaces II: Biological and clinical aspects. *Acta Biomater.* **2014**, *10*, 2907–2918. [CrossRef] [PubMed]
47. Barbosa, T.P.; Naves, M.M.; Menezes, H.H.M.; Pinto, P.H.C.; de Mello, J.D.B.; Costa, H.L. Topography and surface energy of dental implants: A methodological approach. *J. Braz. Soc. Mech. Sci. Eng.* **2017**, *39*, 1895–1907. [CrossRef]
48. Nascimento, R.M.D.; Ramos, S.M.M.; Bechtold, I.H.; Hernandes, A.C. Wettability study on natural rubber surfaces for applications as biomembranes. *ACS Biomater. Sci. Eng.* **2018**, *4*, 2784–2793. [CrossRef]
49. Homma, S.; Makabe, Y.; Sakai, T.; Morinaga, K.; Yokoue, S.; Kido, H.; Yajima, Y. Prospective multicenter non-randomized controlled study on intraosseous stability and healing period for dental implants in the posterior region. *Int. J. Implant Dent.* **2018**, *4*, 10. [CrossRef] [PubMed]
50. Levin, L. Dealing with implant failures. *J. Appl. Oral Sci.* **2008**, *16*, 5. [CrossRef] [PubMed]
51. Gomes, R.Z.; de Vasconcelos, M.R.; Lopes-Guerra, I.M.; de Almeida, R.A.B.; de Campos-Felino, A.C. Implant stability in the posterior maxilla: A controlled clinical trial. *Biomed. Res. Int.* **2017**, *2017*, 6825213. [CrossRef]
52. Tolstunov, L. Implant zones of the jaws: Implant location and related success rate. *J. Implantol.* **2007**, *33*, 10. [CrossRef]